

Theoretical analysis of 17–19-atom metal clusters using many-body potentials†

Lesley D. Lloyd and Roy L. Johnston*

School of Chemistry, University of Birmingham, Edgbaston, Birmingham, UK B15 2TT.
E-mail: roy@tc.bham.ac.uk

Received 5th October 1999, Accepted 29th November 1999

A detailed study is presented of the low-energy isomers for 17–19-atom clusters of Al, Ca, Fe, Ni, Pd and Pt, bound by Murrell–Mottram 2 + 3-body potentials, using a Random Search method. A systematic analysis is also made of isomers formed by removing one or two atoms from the double icosahedron M_{19} cluster geometry. Such “incomplete double icosahedra” are predicted to be the global minima for Pd_{18} , Fe_{18} and Ca_{18} —although the global minima for Fe_{18} and Ca_{18} are different to those previously described. In the cases of Al, Ni and Pt clusters, there are low-lying isomers (or even global minima) which are not derived from the double icosahedron, but rather have four-fold symmetry structures derived from capped Ino decahedra. Comparisons are made between the results obtained for Murrell–Mottram potentials and alternative many-body (Sutton–Chen) and pair (Lennard-Jones and Morse) potentials. Similar structural patterns are observed and differences are found between the various elements for both the Murrell–Mottram and the Sutton–Chen potentials.

1 Introduction

Clusters and nano-particles are of fundamental interest^{1–3} because they occupy a central position between molecules and condensed matter. Theoretical and experimental studies of the size-dependent evolution of the geometric and electronic structures of clusters, and of their chemical and physical properties, is a major area of research. Since clusters have a high percentage of their atoms on the surface there is a strong link between the chemistry and physics of clusters and that of the surfaces of bulk matter. Clusters can also be said to constitute a new type of material, since they often have properties which are fundamentally different from those of discrete molecules or the bulk solid.

Since, for large clusters (of hundreds or thousands of atoms) *ab initio* calculations are at present unfeasible, there has been much interest in developing empirical potentials for the simulation of such species. A recent review of empirical potentials has been presented by Erkoç.⁴ In the present study, empirical 2-plus-3-body Murrell–Mottram potentials⁵ have been applied to the study of clusters of Al, Ca, Fe, Ni, Pd and Pt with 17–19 atoms. Particular attention is paid to clusters derived from the ubiquitous double icosahedral M_{19} structure.

2 The Murrell–Mottram potential

The cluster calculations described here were performed using the Murrell–Mottram (MM) 2 + 3-body potential.^{5,6} The MM potential is based on a many-body expansion of the potential energy:

$$V = V^{(1)} + V^{(2)} + V^{(3)} + \dots V^{(n)} \quad (1)$$

in which the atomic term $V^{(1)}$ is set to zero and the series is truncated at the 3-body level:

$$V = \sum_i \sum_{j>i} V_{ij}^{(2)} + \sum_i \sum_{j>i} \sum_{k>j} V_{ijk}^{(3)} \quad (2)$$

The 2-body (pair) potential is expressed as:

$$V_{ij}^{(2)} = -D(1 + a_2 \rho_{ij}) \exp(-a_2 \rho_{ij}) \quad (3)$$

where D is the dissociation energy of the pair potential, ρ_{ij} is the reduced interatomic distance:

$$\rho_{ij} = (r_{ij} - r_e)/r_e \quad (4)$$

and r_e is the equilibrium distance of the pair potential. The 3-body term:

$$V_{ijk}^{(3)} = D \cdot P(Q_1, Q_2, Q_3) F(a_3, Q_1) \quad (5)$$

is restricted by the requirement that it be unchanged upon interchanging identical atoms. This is achieved by defining the 3-body potential in terms of the symmetry coordinates Q_i :

$$\begin{pmatrix} Q_1 \\ Q_2 \\ Q_3 \end{pmatrix} = \begin{pmatrix} \sqrt{1/3} & \sqrt{1/3} & \sqrt{1/3} \\ 0 & \sqrt{1/2} & -\sqrt{1/2} \\ \sqrt{2/3} & -\sqrt{1/6} & -\sqrt{1/6} \end{pmatrix} \begin{pmatrix} \rho_{ij} \\ \rho_{jk} \\ \rho_{ki} \end{pmatrix} \quad (6)$$

A totally symmetric polynomial can be written in terms of sums and products of the functions: $Q_1, Q_2^2 + Q_3^2, Q_3^3 - 3Q_3Q_2^2$ which are invariant with respect to the interchange of identical atoms. $V^{(3)}$ is defined by an exponent a_3 and a set of polynomial coefficients c_i . The polynomial can be written:

$$P(Q_1, Q_2, Q_3) = c_0 + c_1 Q_1 + c_2 Q_1^2 + c_3 (Q_2^2 + Q_3^2) + c_4 Q_1^3 + c_5 Q_1 (Q_2^2 + Q_3^2) + c_6 (Q_3^3 - 3Q_3 Q_2^2) + c_7 Q_1^4 + c_8 Q_1^2 (Q_2^2 + Q_3^2) + c_9 (Q_2^2 + Q_3^2)^2 + c_{10} Q_1 (Q_3^3 - 3Q_3 Q_2^2) \quad (7)$$

and can either be truncated at the cubic ($c_0 - c_6$) or the quartic ($c_0 - c_{10}$) level. $F(a_3, Q_1)$ is a damping function which makes $V^{(3)}$ go to zero exponentially as Q_1 goes to infinity. Several forms for the damping function have been investigated.⁵ The potentials used in this work have the following damping functions:

† Electronic supplementary information (ESI) available: unrelaxed and relaxed M_{17} IDI isomers. See <http://www.rsc.org/suppdata/dt/a9/a908003a/>

Table 1 MM potentials for the metals studied in this work

Coefficient	Al	Ca	Fe	Ni	Pd	Pt
a_2	7	6	6.55	8.5	7	8.5
a_3	8	11.5	9.6	10	10.2	9
D/eV	0.9073	0.3799	0.8847	1.189	0.946	1.613
$r_e/\text{\AA}$	2.7568	3.9372	2.8632	2.394	2.667	2.699
c_0	0.2525	0.1174	0.1760	0.226	0.197	0.244
c_1	-0.4671	1.7882	1.7958	-0.018	-0.221	-0.429
c_2	4.4903	10.1597	5.0885	5.334	6.516	5.814
c_3	-1.1717	1.1767	-2.9047	-2.856	-0.435	-2.581
c_4	1.6498	12.7462	-2.2007	-1.294	10.273	1.268
c_5	-5.3579	-16.7545	-6.1349	-0.380	-14.543	-7.386
c_6	1.6327	7.9449	2.8605	2.381	4.463	5.401
c_7		56.6397	13.2511			
c_8		13.9832	-8.3421			
c_9		-27.2585	4.5088			
c_{10}		33.6836	-0.5679			
F	sech	tanh	exp	sech	sech	sech
Ref.	7	8	9	10	11	11

$$\begin{aligned}
 F(a_3, Q_1) &= \exp(-a_3 Q_1) && \text{exponential} \\
 F(a_3, Q_1) &= \frac{1}{2} \left(1 - \tanh\left(\frac{a_3 Q_1}{2}\right) \right) && \tanh \\
 F(a_3, Q_1) &= \text{sech}(a_3 Q_1) && \text{sech}
 \end{aligned} \quad (8)$$

The parameters defining the MM potentials for the elements studied here are listed in Table 1.^{7–11} These potentials have been derived by fitting experimental structural, energetic and lattice dynamical data of the corresponding bulk solids.⁵

3 Cluster energetics

From eqn. (2), the total potential energy (V_{clus}) of an N -atom cluster, bound by the 2 + 3-body MM potential, is given by:

$$V_{\text{clus}} = \sum_i^{N-1} \sum_{j>i}^N V_{ij}^{(2)} + \sum_i^{N-2} \sum_{j>i}^{N-1} \sum_{k>j}^N V_{ijk}^{(3)} \quad (9)$$

and the *average binding energy* (i.e. the binding energy per atom) is defined as:

$$E_b = \frac{-V_{\text{clus}}}{N} \quad (10)$$

A measure of the contribution of an individual atom (i) to the total binding energy of the cluster is given by the *partial binding energy*:

$$\varepsilon_b(i) = - \left[\frac{1}{2} \sum_j' V_{ij}^{(2)} + \frac{1}{3} \sum_j' \sum_{k>j}' V_{ijk}^{(3)} \right] \quad (11)$$

where the prime indicates summation over all atoms except i and the factors of $\frac{1}{2}$ and $\frac{1}{3}$ arise because pair and 3-body terms have to be shared between all atoms contributing to them. The average binding energy is regained as:

$$E_b = \sum_i \varepsilon_b(i) / N \quad (12)$$

When considering the energy of clusters isomers formed by removing atoms from a given parent cluster, one must consider the *atom removal energy*. The energy required to remove atom (i) from an N -atom cluster, $\varepsilon_r(i)$, is equal to the difference in the total energies of the parent cluster and the unrelaxed ($N - 1$)-atom derivative:

$$\varepsilon_r(i) = -[V_{\text{tot}}(N) - V_{\text{tot}}^u(N - 1)] \quad (13)$$

where the superscript (u) indicates that the ($N - 1$)-atom cluster

is unrelaxed. (It should be noted that the atom removal energy is not the activation energy for the actual removal of an atom from an N -vertex cluster). Rewriting eqn. (13) in terms of the pair and 3-body contributions to the total energy:

$$\varepsilon_r(i) = - \left[\sum_{j \neq i} V_{ij}^{(2)} + \sum_{j \neq i} \sum_{k > j} V_{ijk}^{(3)} \right] \quad (14)$$

Comparing this expression with that (eqn. (11)) for the partial binding energies, (ε_b), it is apparent that, in ε_r , the 2- and 3-body terms are not multiplied by the factors $\frac{1}{2}$ and $\frac{1}{3}$ respectively. This is because, when calculating the energy required to remove an atom entirely from a cluster, all the interactions involving that atom must be broken, and the energy is not shared among the atoms remaining. For a pair-only potential (such as the Lennard-Jones or Morse potentials), the following relationship holds:

$$\varepsilon_r(i) = 2 \times \varepsilon_b(i) \quad (15)$$

For the 2-plus-3-body MM potential, however, the fact that eqns. (11) and (14) have different weightings of the 2- and 3-body contributions means that there is no simple proportionality between ε_r and ε_b . This also implies that the most stable ($N - 1$)-atom isomer, formed by removing an atom from a given N -atom cluster, need not necessarily correspond to the loss of the atom of lowest ε_b . The same arguments apply to any many-body potential of order equal to or higher than the MM potential. Finally, though we have only discussed the unrelaxed ($N - 1$)-vertex isomers, the order of stability of these isomers may be changed by the relaxation process.

Cluster calculations were performed using the program CLUSPRO97.^{12–14} The program optimises cluster geometries, which may be randomly generated, fragments of bulk solids or polyhedral shells, using a variety of Quasi-Newton, conjugate gradient and Monte Carlo algorithms. Vibrational frequencies are also calculated to identify any saddle points (the order of a saddle point is equal to the number of imaginary vibrational frequencies).

4 Isomers based on the M_{19} double icosahedron

In previous studies of MM clusters of Fe, Ca and Sr,^{13,14} the global minima (GM) (or at least the lowest energy structures that were found) for the 18- and 17-atom clusters were related to the double icosahedron—the GM for 19 atoms (Fig. 1) by the removal of one and two atoms, respectively. We have recently found, however, that the MM potential for Al does not yield these incomplete double icosahedra (IDI) structures among the top five most stable isomers for either nuclearity.¹⁵ Rather than

Table 2 Coordination numbers of different atom sites in the double icosahedron

Atom site	n_a	CN
A	2	12
B	5	8
C	10	6
D	2	6

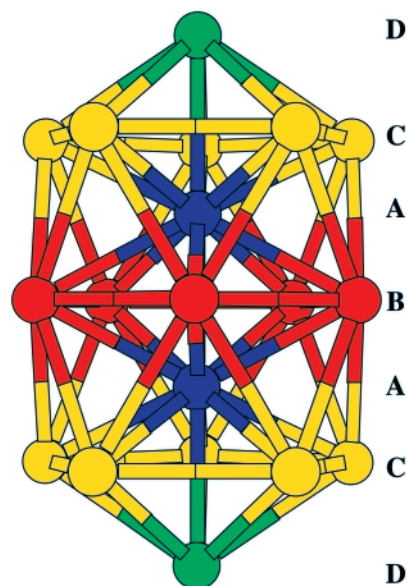


Fig. 1 Sets of symmetry-equivalent atoms in the M_{19} double icosahedral cluster.

drawing out and inspecting all of the many minima found for Al_{17} and Al_{18} , in an attempt to find the IDI isomers, we decided to perform a more systematic study of the stabilities of IDI isomers for Al. In order to investigate the effect of changing the MM potential on the relative stabilities of IDI isomers, this study was extended to include a number of other metals: Fe, Ca, Ni, Pd and Pt. As mentioned above, preliminary studies of Fe and Ca clusters have already been made,^{13,14} but no systematic study has been carried out on IDI isomers of these metals.

4.1 Generation of isomers

As shown in Fig. 1, the double icosahedron comprises four sets of symmetry-equivalent atoms, which are labelled A–D in the figure. The numbers of atoms in each set (n_a) are listed in Table 2, along with their coordination numbers (CN). An 18-vertex IDI is generated by removing an atom from one of the sets A–D of the relaxed DI (double icosahedron). There are therefore four geometrically distinct M_{18} isomers that can be formed by removing an atom from the M_{19} DI (obviously, it does not matter which of the atoms in a given set is removed, since the resulting clusters are geometrically equivalent). These isomers are shown in Fig. 2, along with the parent M_{19} structure. The 18-vertex isomers are labelled $M_{18}(X)$, where X represents the type of atom (A–D) that has been removed to generate the IDI.

There are 20 geometrically distinct 17-vertex isomers which can be generated by the removal of two vertices from the double icosahedron. These isomers are also shown in Fig. 2. The 17-vertex isomers are labelled $M_{17}(XYn)$, where X and Y represent the types of atoms (A–D) that have been removed and n (where applicable) is a number which distinguishes between different isomers with the same {X, Y} descriptors. The lower the n value, the closer (in terms of intervening bonds) the “vacancies” (*i.e.* the missing vertices). Thus, the isomer $M_{17}(AD1)$ has the central atom (type A) of one icosahedron and the on-axis capping atom (type D) of the same icosahedron miss-

Table 3 Partial binding energies (eV) of different atoms in the Al_{19} double icosahedron

Atom site	$\epsilon_b(i)$	$\epsilon_r(i)$
A	1.9541	3.1194
B	1.4159	2.4233
C	1.1076	1.9410
D	1.0905	1.9129

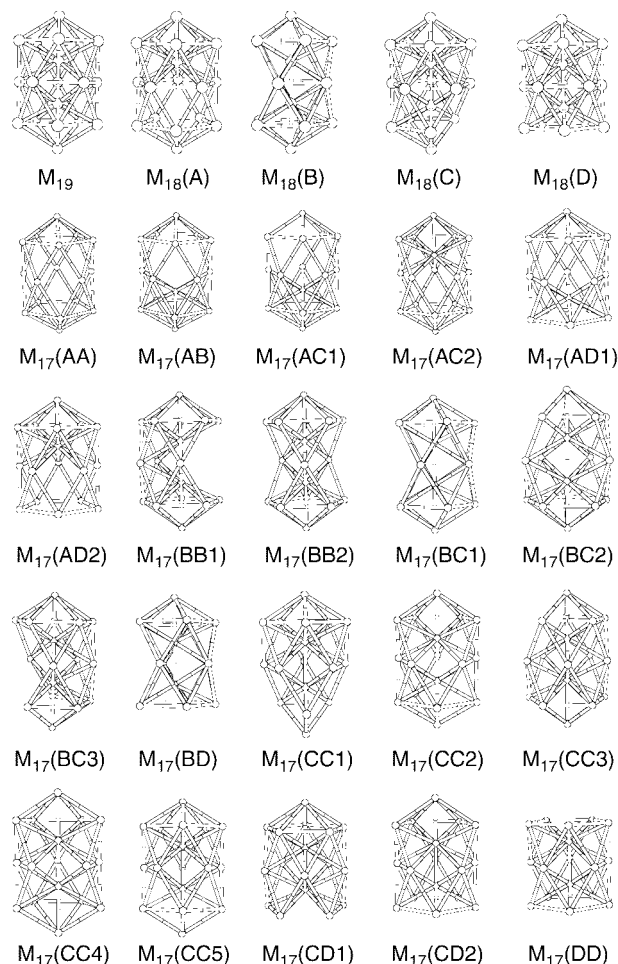


Fig. 2 M_{18} and M_{17} derivatives of the M_{19} double icosahedron.

ing. In the isomer $M_{17}(AD2)$, however, the D-type atom is missing from the centred, rather than the uncentred icosahedron.

5 Al clusters

5.1 Results for Al_{18}

Considering the relative stabilities of the four 18-vertex isomers, one might suppose that the most stable isomer would be generated by removing the atom which has the lowest partial binding energy, ϵ_b . While this is generally found to be the case, the energy of the unrelaxed IDI cluster depends on the atom removal energy, ϵ_r . The values of ϵ_b and ϵ_r , for the four sets of symmetry equivalent atoms (A–D) of the double icosahedron Al_{19} , are listed in Table 3.

These values show that, for the process of removing an atom from DI Al_{19} , the atom removal energies are in the same order [$\epsilon_r(A) > \epsilon_r(B) > \epsilon_r(C) > \epsilon_r(D)$] as the partial binding energies. This ordering follows the order of decreasing coordination number [CN(A) > CN(B) > CN(C) = CN(D)] evident from Table 2, showing the importance of the nearest neighbours in determining the stabilities of cluster isomers. (This reflects the dominant contribution of the pair component to the MM

Table 4 Unrelaxed and relaxed binding energies and relaxation energies (eV) of Al₁₈ isomers generated by the removal of a single atom from the double icosahedron

Atom removed	E_b^u	E_b^r	ΔE_b^r
A	2.0955	2.1348	0.0393
B	2.1094	2.1122	0.0028
C	2.1407	2.1441	0.0034
D	2.1427	2.1455	0.0028

potential.) The small difference between $\varepsilon_r(\text{C})$ and $\varepsilon_r(\text{D})$ is due to their equal coordination numbers, but also reflects the fact that the C-type atoms have interactions of the type CC' (between eclipsed atoms in the upper and lower rings), which the more peripheral D atoms do not possess. The observed ε_r ordering means that the lowest energy (unrelaxed) 18-vertex isomer will result from the removal of a D-type capping atom and the highest (least stable) from the removal of an A-type interstitial atom. This is confirmed by the calculated average binding energies of the unrelaxed isomers (as listed in Table 4), which are in the order $E_b^u(\text{D}) > E_b^u(\text{C}) > E_b^u(\text{B}) > E_b^u(\text{A})$. The label (X) again refers to the cluster with an atom of type X missing. Unrelaxed geometries were generated by removing a vertex from the relaxed Al₁₉ double icosahedron, while keeping the coordinates of all other atoms constant. The 18-atom IDI were subsequently relaxed using the Quasi-Newton NAG routine EQ4KAF.¹⁶

The average binding energies of the relaxed Al₁₈ isomers (E_b^r) are listed in Table 4 along with the relaxation energies:

$$\Delta E_b^r = E_b^r - E_b^u \quad (16)$$

The relaxation energies of the Al₁₈(X) isomers (for X = B, C, D) are all very small (less than 0.2% of E_b^u) and the geometrical changes upon relaxation are correspondingly small for these isomers. On the other hand, the least stable (unrelaxed) isomer Al₁₈(A) (which has an interstitial atom removed) relaxes by nearly 2%—i.e. an order of magnitude greater relaxation than for the other three isomers—and there is a more significant change in the geometry upon relaxation. This large relaxation is clearly necessary to compensate for the removal of a 12-coordinate atom. In fact, the relaxation of the A-isomer is so large that the relaxed Al₁₈(A) cluster becomes the third most stable IDI isomer for Al₁₈, with the order of binding energies of the relaxed clusters being $E_b^r(\text{D}) > E_b^r(\text{C}) > E_b^r(\text{A}) > E_b^r(\text{B})$.

After relaxation, the most stable of the IDI isomers is still Al₁₈(D) (which has one of the capping atoms on the 5-fold axis missing) but its binding energy (2.1455 eV) is considerably lower than the global minimum (GM) previously found for Al₁₈ (2.1618 eV).¹⁵ This study also confirms that none of the IDI are among the five most stable isomers for Al₁₈ ($E_b[\text{Al}_{18}(5)] = 2.1585$ eV). Subsequent checking of the output from a multiple random search procedure,¹⁵ and drawing the clusters with energies matching those calculated for the relaxed IDIs, revealed that the four 18-vertex IDI isomers can indeed be found by the random search method. The 18-vertex global minima found for the Lennard-Jones and (medium-ranged) Morse potentials^{17,18} have the Al₁₈(D) structure, which is consistent with our finding that the pair component of the MM potential favours removal of the capping D atom. The (assumed) global minima previously found for Ca₁₈ and Sr₁₈¹⁴ had the M₁₈(D) geometry, while Fe₁₈ was found to adopt the Al₁₈(C) geometry.¹³ Since the search undertaken for the GM in these previous studies was not as rigorous as in the more recent work,¹⁵ it is possible that the true GM were missed. A more systematic study of the IDI M₁₈ isomers for these and a number of other metals is presented below.

Table 5 Unrelaxed and relaxed binding energies and relaxation energies (eV) of Al₁₇ isomers generated by the removal of two atoms from the double icosahedron

Atoms removed	E_b^u	E_b^r	ΔE_b^r
AA	1.9661	2.0412	0.0751
AB	1.9906	—	—
AC1	2.0254	2.1142	0.0888
AC2	2.0373	2.0783	0.0410
AD1	2.0409	2.0774	0.0365
AD2	2.0268	2.1235	0.0967
BB1	2.0186	2.0386	0.0200
BB2	2.0183	2.0228	0.0045
BC1	2.0651	2.0873	0.0222
BC2	2.0518	2.0576	0.0058
BC3	2.0532	2.0575	0.0043
BD	2.0543	2.0587	0.0044
CC1	2.0852	2.0879	0.0027
CC2	2.0981	2.1189	0.0208
CC3	2.0860	2.0937	0.0070
CC4	2.0864	2.0926	0.0062
CC5	2.0866	2.0928	0.0062
CD1	2.0888	2.0938	0.0050
CD2	2.1004	2.1252	0.0248
DD	2.0910	2.0944	0.0034

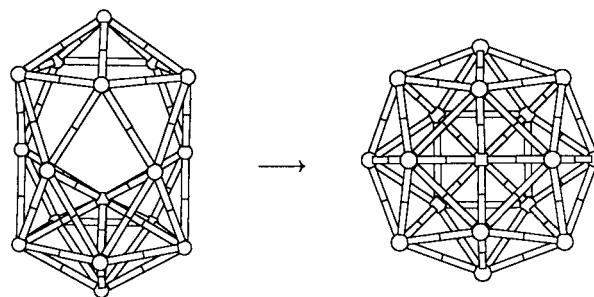


Fig. 3 Relaxation of the Al₁₇(AB) IDI isomer (left) to the Al₁₇ global minimum (right).

5.2 Results for Al₁₇

The unrelaxed (E_b^u) and relaxed (E_b^r) binding energies, and the relaxation energies (ΔE_b^r), are listed in Table 5, for the 20 IDI isomers of Al₁₇ (see Fig. 2). Prior to relaxation, the least stable IDI isomer is Al₁₇(AA) ($E_b^u = 1.9661$ eV), which has both (12-coordinate) interstitial atoms missing. The most stable IDI isomer is Al₁₇(CD2) ($E_b^u = 2.1004$ eV), rather than the (DD) isomer, which might have been expected on the basis of the results for Al₁₈. In fact, Al₁₇(DD) has the third highest binding energy of the unrelaxed IDI isomers.

Table 5 reveals that there is a wide range of relaxation energies—from 0.0027 eV for Al₁₇(CC1) to 0.0967 eV for Al₁₇(AD2). The reason why there is no E_b^r value reported for Al₁₇(AB) is that this isomer relaxed to the non-IDI global minimum for Al₁₇ as shown in Fig. 3. This indicates that there is no energy barrier to prevent the unrelaxed (AB) isomer rearranging to the GM, though it does not exclude the possibility of a relaxed metastable IDI isomer with the Al₁₇(AB) geometry, which could perhaps be found by using an alternative minimisation routine, or by performing a rigorous grid search of the potential energy surface. The most stable isomer after relaxation is still Al₁₇(CD2) and its binding energy ($E_b^r = 2.1252$ eV) is confirmed to be well outside the range of the five most stable isomers found by the previous random search ($E_b = 2.1320$ – 2.1354 eV).¹⁵

6 Analysis of M₁₇ and M₁₈ isomers (M = Al, Ca, Fe, Ni, Pd, Pt)

The procedure described above was repeated to study the alkaline-earth metal calcium and the Group 10 transition

Table 6 Unrelaxed and relaxed binding energies and relaxation energies (eV) of M_{18} isomers generated by the removal of a single atom from the double icosahedron

	Al E_b^u	Al E_b^r	Al ΔE_b^r	Ca E_b^u	Ca E_b^r	Ca ΔE_b^r	Fe E_b^u	Fe E_b^r	Fe ΔE_b^r
A	2.0955	2.1348	0.0393	1.0691	1.0760	0.0069	2.3500	2.3613	0.0113
B	2.1094	2.1122	0.0028	1.1081	1.1098	0.0017	2.3812	2.3816	0.0004
C	2.1407	2.1441	0.0034	1.1319	1.1337	0.0018	2.4315	2.4320	0.0005
D	2.1427	2.1455	0.0028	1.1309	1.1330	0.0021	2.4328	2.4336	0.0008
	Ni E_b^u	Ni E_b^r	Ni ΔE_b^r	Pd E_b^u	Pd E_b^r	Pd ΔE_b^r	Pt E_b^u	Pt E_b^r	Pt ΔE_b^r
A	2.7376	2.7689	0.0313	2.3027	2.3369	0.0342	3.6067	3.7394	0.1327
B	2.7405	2.7428	0.0023	2.3329	2.3354	0.0025	3.6252	3.6335	0.0083
C	2.7858	2.7891	0.0033	2.3754	2.3793	0.0039	3.6834	3.7173	0.0339
D	2.7853	2.7892	0.0039	2.3762	2.3801	0.0039	3.6865	3.6991	0.0126

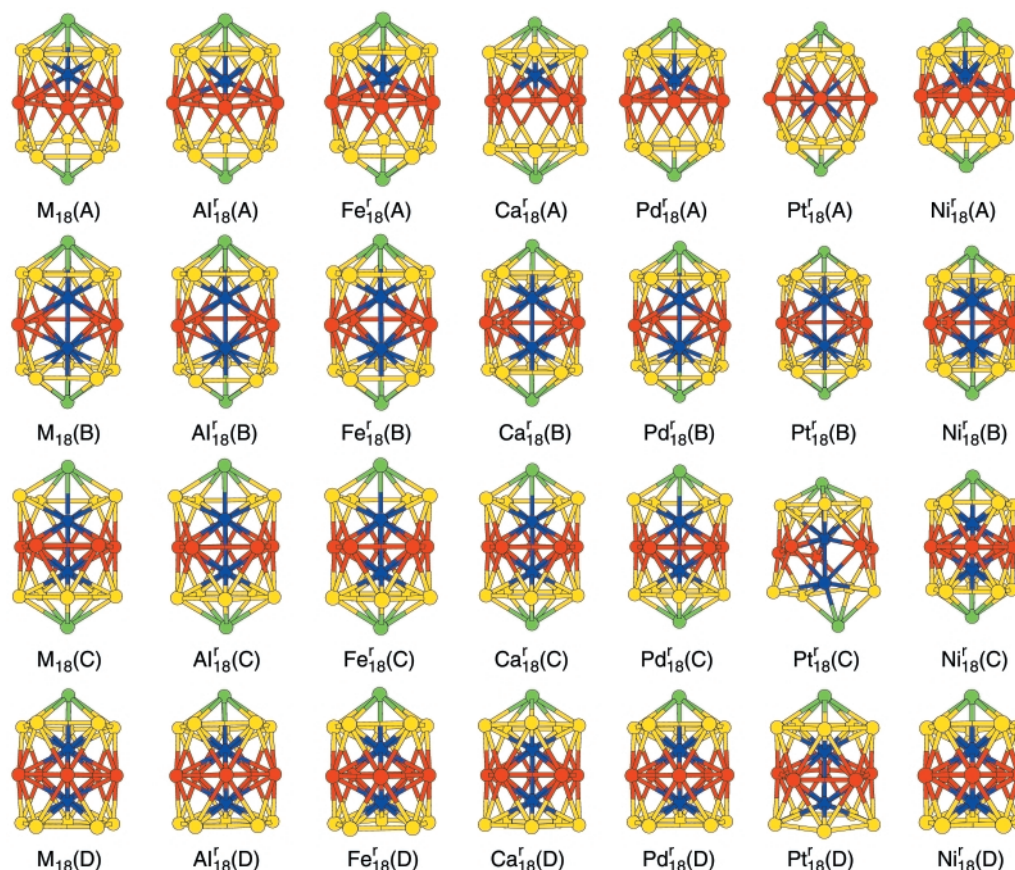


Fig. 4 Isomers obtained by relaxation of M_{18} IDI ($M = \text{Al, Ca, Fe, Ni, Pd}$ and Pt).

metals nickel, palladium and platinum. These are all fcc in the bulk. The transition metal, iron, which is bcc in the bulk was also studied.

6.1 M_{18} Isomers

The symmetry equivalent sets of atoms (A–D) in an M_{19} DI cluster are colour coded in Fig. 1. This colour coding is important for monitoring rearrangements accompanying relaxation.

Values of E_b^u , E_b^r and ΔE_b^r for the various IDI M_{18} isomers, before and after relaxation, are listed in Table 6. Fig. 4 shows the unrelaxed IDI isomers $M_{18}(X)$ (first column) together with the structures $M_{18}^r(X)$ generated by relaxation for $M = \text{Al, Fe, Ca, Ni, Pd}$ and Pt .

In most cases, the geometries of the clusters did not alter significantly upon relaxation. The exception was Pt, where $\text{Pt}_{18}(\text{A})$ and $\text{Pt}_{18}(\text{C})$ underwent significant rearrangements, yielding non-IDI isomers. In $\text{Pt}_{18}^r(\text{A})$ the remaining A-atom has moved into the centre of the cluster and a more symmetrical cluster results. In the case of $\text{Pt}_{18}^r(\text{C})$, the rearrangement is

smaller, corresponding to the breaking of four bonds (AC, CC, A_2C and DC) of the IDI isomer. The changes in geometry of the Pt clusters are reflected in Table 6 which is a comparison of the relaxation energies for the metals investigated. $\text{Pt}_{18}^r(\text{A})$ has the largest relaxation energy (0.1327 eV), while ΔE_b^r for $\text{Pt}_{18}^r(\text{C})$ (0.0339 eV) is also relatively high.

Table 7 lists the order of stability of the M_{18} IDI clusters before and after relaxation. After relaxation $M_{18}(\text{D})$ is the most stable for Al, Fe, Pd and Ni; $M_{18}(\text{C})$ for Ca; and $M_{18}(\text{A})$ for Pt. The order of $M_{18}(\text{A})$ and $M_{18}(\text{B})$ is swapped for Al and Pd after relaxation, for Fe and Ca the order remains the same. The fully relaxed binding energies for the five most stable isomers are listed in Table 8 and these clusters are illustrated in Fig. 5.

For each of the metals studied, 1000 random searches were performed in order to identify the five most stable (highest E_b values) M_{18} isomers. The Random Search method has been discussed in detail elsewhere.¹⁵ Three of the IDI M_{18} clusters, $\text{Pd}_{18}(\text{D})$, $\text{Fe}_{18}(\text{D})$ and $\text{Ca}_{18}(\text{C})$ were found to be global minima, while $\text{Pd}_{18}(\text{C})$, $\text{Fe}_{18}(\text{C})$ and $\text{Ca}_{18}(\text{D})$ were the second most stable clusters. None of the other IDI clusters featured among the five

Table 7 Order of stability before and after relaxation for IDI M_{18} isomers (A represents $M_{18}(A)$ etc.)

M_{18}	Unrelaxed	Relaxed
Al	D > C > B > A	D > C > A > B
Fe	D > C > B > A	D > C > B > A
Ca	C > D > B > A	C > D > B > A
Ni	C > D > B > A	D > C > A > B
Pd	D > C > B > A	D > C > A > B
Pt	D > C > B > A	A > C > D > B

Table 8 Binding energies (eV) of the five most stable isomers found for M_{18}

M_{18}	Isomer				
	1 (GM)	2	3	4	5
Al	2.1618	2.1596	2.1588	2.1586	2.1585
Fe	2.4336	2.4320	2.4059	2.4049	2.4047
Ca	1.1337	1.1330	1.1206	1.1205	1.1202
Ni	2.8117	2.8101	2.8047	2.8041	2.8025
Pd	2.3801	2.3793	2.3716	2.3696	2.3654
Pt	3.7609	3.7553	3.7532	3.7526	3.7524

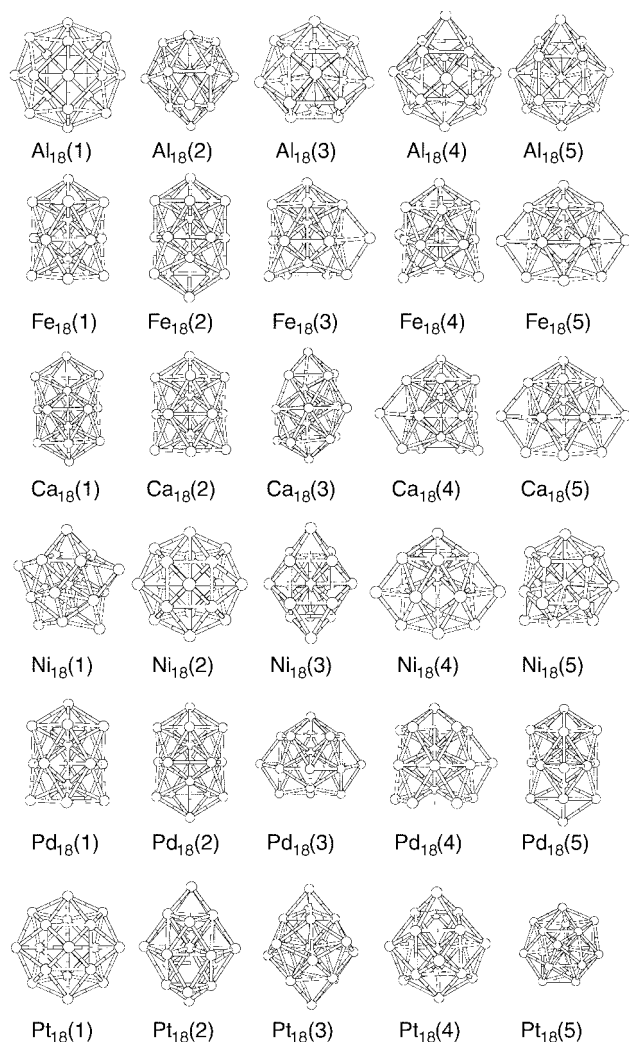


Fig. 5 The five most stable isomers found for M_{18} (M = Al, Ca, Fe, Ni, Pd and Pt).

most stable isomers, though all of the M_{18} IDI isomers were found by the Random Search method. It should be noted that in previous studies of Fe and Ca clusters using MM potentials,^{13,14} the GM for the M_{18} clusters were reported to be

$Fe_{18}(C)$ and $Ca_{18}(D)$. These assignments can now be seen to be incorrect as the more rigorous study reported here indicates that $Fe_{18}(D)$ and $Ca_{18}(C)$ are definitely the most stable IDI isomers. The more extensive Random Search in the present study means that it is very likely that these are actually the GM for Fe_{18} and Ca_{18} using the MM potential.

The geometries of the Al and Pt GM for $N=18$ are the same—namely the C_{4v} -symmetry structure generated by distorting a pentacapped Ino decahedron such that an edge opposite to one of the square-face-capping atoms is broken. This distortion has been described in detail in a previous paper.¹⁵ Interestingly, the GM for Ni_{18} is an undistorted pentacapped Ino decahedron, with D_{5h} symmetry, while the second most stable isomer has the distorted-decahedral C_{4v} structure. Similar structures have been found for silver and gold clusters bound with MM potentials.^{19,20}

6.2 M_{17} Isomers

Values of E_b^u , E_b^r and ΔE_b^r for the 20 distinct M_{17} IDI isomers (M = Al, Ca, Fe, Ni, Pd and Pt) are listed in Table 9. A figure, showing the unrelaxed IDI isomers and the geometries to which they relax, for each metal, is available as Electronic Supplementary Information.

Compared with the M_{18} isomers, the IDI isomers of M_{17} generally undergo larger relaxations (as evidenced by larger ΔE_b^r values) and many more of these relaxations involve structural rearrangements. The geometry of the $M_{17}(AA)$ isomer of Fe, Ca and Pd changes significantly on relaxation. $Fe_{17}(AA)$ and $Pd_{17}(AA)$ relax to a structure (see Fig. 3) with four-fold symmetry (D_{4d}), which has been found for all these metals and is actually the global minimum for Al_{17} .¹⁵ The relaxed $Ca_{17}(AA)$ structure is very similar to the D_{4d} cluster but the B atom is slightly off-centre. These changes in geometry are reflected in the high ΔE_b^r values 0.1790 eV, 0.0975 eV and 0.1922 eV for Fe, Ca and Pd respectively. Pt also shows a substantial difference in energy after relaxation, this is because of the compression of the whole structure, although the geometry is unchanged. The D_{4d} isomer (the GM for Al_{17}) is also produced by the relaxation of $Al_{17}(AB)$, $Ni_{17}(AB)$ and $Pd_{17}(AB)$, while $Ca_{17}(AB)$ relaxes to the same structures as $Ca_{17}(AA)$.

The five most stable isomers found for M_{17} , after 1000 random searches, are shown in Fig. 6 and their binding energies are listed in Table 10. For Al_{17} , as mentioned above, the D_{4d} structure is the GM and none of the unreconstructed IDI isomers are among the five most stable isomers. For Fe and Ca, the GM are IDI isomers, $Fe_{17}(CD2)$ and $Ca_{17}(CC2)$, with additional IDI isomers also being among the five most stable isomers. The Ca_{17} GM was correctly identified in a previous study,¹⁴ but the second most stable Fe_{17} isomer [$Fe_{17}(2)$] was previously incorrectly reported as the GM for Fe_{17} .¹³ For Pd, the IDI isomers $Pd_{17}(CD2)$ and $Pd_{17}(CC2)$ are the second and fourth most stable isomers respectively. For Ni and Pt, however, none of the IDI isomers are among the five most stable. The D_{4d} structure is the GM for Pt and the second most stable isomer for Ni. The GM for Ni_{17} is a tetracapped Ino decahedron, and is therefore derived by removing a (square-face) capping atom from $Ni_{18}(1)$.

Considering the D_{4d} M_{17} isomer, which is the GM for Al_{17} and Pt_{17} and the second most stable isomer for Ni_{17} , it is interesting to analyse how this structure (which is related to the C_{4v} isomer found for the M_{18} clusters by the removal of one of the capping atoms on the four-fold symmetry axis) can be formed by the relaxation of IDI M_{17} isomers. The D_{4d} isomer can be found after minimisation from different starting points, as shown in Fig. 7. Starting from the hollow $M_{17}(AA)$ structure, the D_{4d} isomer is obtained for M = Fe and Pd. In both cases, one of the central ring (B) atoms moves into the centre and there is a large rearrangement. The D_{4d} isomer is also generated by relaxing the $M_{17}(AB)$ isomer for Al, Pd and Ni. In all cases the remaining A atom becomes the central atom in the D_{4d}

Table 9 Unrelaxed and relaxed binding energies and relaxation energies (eV) of M_{17} isomers generated by the removal of two atoms from the double icosahedron

	Al E_b^u	Al E_b^r	Al ΔE_b^r	Fe E_b^u	Fe E_b^r	Fe ΔE_b^r	Ca E_b^u	Ca E_b^r	Ca ΔE_b^r
AA	1.9661	2.0412	0.0751	2.1692	2.3482	0.1790	0.9570	1.0545	0.0975
AB	1.9906	2.1354	0.1448	2.2149	2.3510	0.1361	1.0084	1.0545	0.0461
AC1	2.0254	2.1142	0.0888	2.2690	2.3790	0.1100	1.0359	1.1117	0.0758
AC2	2.0373	2.0783	0.0410	2.2667	2.2788	0.0121	1.0247	1.0315	0.0068
AD1	2.0409	2.0774	0.0365	2.2676	2.2812	0.0136	1.0254	1.0321	0.0067
AD2	2.0268	2.1235	0.0967	2.2716	2.3813	0.1097	1.0352	1.1109	0.0757
BB1	2.0186	2.0386	0.0200	2.2559	2.2575	0.0016	1.0527	1.0570	0.0043
BB2	2.0183	2.0228	0.0045	2.2460	2.2468	0.0008	1.0408	1.0718	0.0310
BC1	2.0651	2.0873	0.0222	2.2996	2.3009	0.0013	1.0799	1.0845	0.0046
BC2	2.0518	2.0576	0.0058	2.3194	2.3224	0.0030	1.0663	1.0688	0.0025
BC3	2.0532	2.0575	0.0043	2.2998	2.3009	0.0011	1.0679	1.0707	0.0028
BD	2.0543	2.0587	0.0044	2.3012	2.3030	0.0018	1.0653	1.0683	0.0030
CC1	2.0852	2.0879	0.0027	2.3531	2.3540	0.0009	1.0915	1.0936	0.0021
CC2	2.0981	2.1189	0.0208	2.3531	2.3541	0.0010	1.1067	1.1117	0.0050
CC3	2.0860	2.0937	0.0077	2.3744	2.3790	0.0046	1.0929	1.0968	0.0039
CC4	2.0864	2.0926	0.0062	2.3539	2.3550	0.0011	1.0933	1.0965	0.0032
CC5	2.0866	2.0928	0.0062	2.3530	2.3540	0.0010	1.0935	1.0968	0.0033
CD1	2.0888	2.0938	0.0050	2.3543	2.3556	0.0013	1.0924	1.0961	0.0037
CD2	2.1004	2.1252	0.0248	2.3761	2.3813	0.0052	1.1058	1.1109	0.0051
DD	2.0910	2.0944	0.0034	2.3557	2.3571	0.0014	1.0912	1.0952	0.0040

	Ni E_b^u	Ni E_b^r	Ni ΔE_b^r	Pd E_b^u	Pd E_b^r	Pd ΔE_b^r	Pt E_b^u	Pt E_b^r	Pt ΔE_b^r
AA	2.5753	2.6248	0.0495	2.1298	2.3220	0.1922	3.3726	3.5214	0.1488
AB	2.5958	2.7758	0.1800	2.1786	2.3220	0.1434	3.4229	3.7017	0.2788
AC1	2.6443	2.7585	0.1142	2.2248	2.3428	0.1180	3.4833	3.6891	0.2058
AC2	2.6582	2.6901	0.0319	2.2284	2.2623	0.0339	3.5039	3.7017	0.1978
AD1	2.6439	2.7655	0.1216	2.2312	2.2630	0.0318	3.5100	3.7017	0.1917
AD2	2.6595	2.6898	0.0303	2.2252	2.3452	0.1200	3.4850	3.6935	0.2085
BB1	2.6168	2.6448	0.0280	2.2236	2.2447	0.0211	3.4661	3.5291	0.0630
BB2	2.6140	2.6165	0.0025	2.2155	2.2182	0.0027	3.4617	3.4699	0.0082
BC1	2.6812	2.7174	0.0362	2.2800	2.2938	0.0138	3.5499	3.6180	0.0681
BC2	2.6622	2.6673	0.0051	2.2608	2.2656	0.0048	3.5236	3.7084	0.1848
BC3	2.6642	2.6688	0.0046	2.2624	2.2667	0.0043	3.5265	3.7165	0.1900
BD	2.6618	2.6663	0.0045	2.2617	2.2661	0.0044	3.5271	3.5394	0.0123
CC1	2.7103	2.7128	0.0025	2.3059	2.3084	0.0025	3.5851	3.5922	0.0071
CC2	2.7313	2.7585	0.0272	2.3261	2.3428	0.0167	3.6123	3.6770	0.0647
CC3	2.7117	2.7188	0.0071	2.3072	2.3156	0.0084	3.5873	3.6233	0.0360
CC4	2.7125	2.7182	0.0057	2.3075	2.3142	0.0067	3.5885	3.6090	0.0205
CC5	2.7128	2.7187	0.0059	2.3076	2.3142	0.0066	3.5888	3.6098	0.0210
CD1	2.7304	2.7655	0.0351	2.3048	2.3149	0.0101	3.5922	3.6109	0.0187
CD2	2.7122	2.7184	0.0062	2.3268	2.3452	0.0184	3.6150	3.6935	0.0785
DD	2.7117	2.7174	0.0057	2.3093	2.3151	0.0058	3.5956	3.6093	0.0137

Table 10 Binding energies (eV) of the five most stable isomers found for M_{17}

M_{17}	Isomer				
	1 (GM)	2	3	4	5
Al	2.1354	2.1337	2.1333	2.1328	2.1320
Fe	2.3813	2.3809	2.3804	2.3790	2.3643
Ca	1.1117	1.1109	1.1108	1.1098	1.0968
Ni	2.7784	2.7758	2.7747	2.7709	2.7699
Pd	2.3490	2.3452	2.3441	2.3428	2.3359
Pt	3.7165	3.7102	3.7090	3.7084	3.7075

cluster. Finally, the $Pt_{17}(BC3)$ cluster relaxes to the D_{4d} structure with one of the A atoms becoming the central atom. While the D_{4d} isomer was also found for Fe and Pd, inspection of Fig. 6 shows that this structure is not among the five most stable isomers. As mentioned above, for Ca, the $M_{17}(AA)$ and $M_{17}(AB)$ IDI both relax to give the same structure, which is a distorted form of the D_{4d} isomer, with the interstitial atom shifted off-centre and an extra bond formed across one of the square faces.

7 The most stable isomers of M_{19}

In order to complete this study of isomer stability for MM

clusters, and for comparison with our previous work on Al,¹⁵ 1000 random searches were performed for M_{19} . The five most stable isomers found for M_{19} clusters of Al, Fe, Ca, Ni, Pd and Pt are shown in Fig. 8 and their binding energies are listed in Table 11. The double icosahedron is the GM for M_{19} for all the metals, except Pt, which has a GM with a D_{4d} structure—the second most stable structure for Al and Ni.

Inspection of Figs. 5, 6 and 8 reveals that there is a pattern which links the structures of certain isomers of M_{17} – M_{19} . Considering Al first of all, the GM for $N = 17$ [$Al_{17}(1)$] has D_{4d} symmetry, with a 4-fold rotation axis (parallel to the viewing axis in Fig. 6) passing through two opposite square faces. The GM for $N = 18$ [$Al_{18}(1)$] is generated from $Al_{17}(1)$ by capping one of the square faces, to generate a structure with C_{4v} symmetry. Capping the second square face gives rise to the structure [$Al_{19}(2)$ —with D_{4d} symmetry] which is the second most stable isomer for Al_{19} . The structure of this M_{19} isomer and its M_{18} and M_{17} derivatives (formed by removing one or two square-face-capping atoms from the fourfold-rotation axis) has been discussed previously.¹⁵

8 Comparison with other potentials

8.1 The Sutton–Chen potential

The Sutton–Chen (SC) potential²¹ provides a reasonable description of various bulk properties with an implicit many-

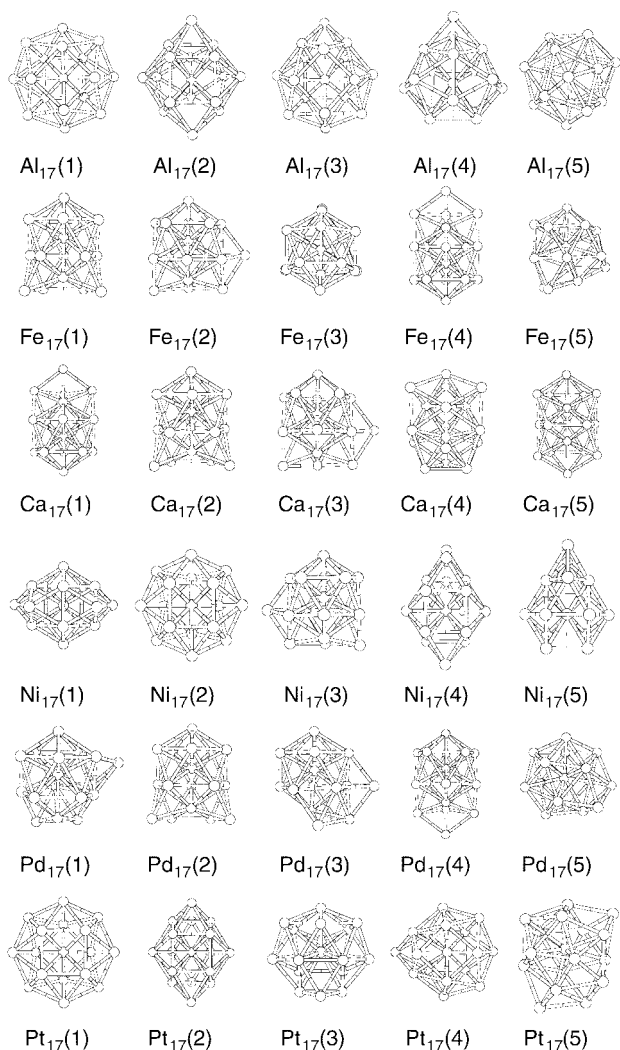


Fig. 6 The five most stable isomers found for M_{17} ($M = \text{Al, Ca, Fe, Ni, Pd}$ and Pt).

body representation of the delocalised metallic bonding. However it does not include any directional terms and these are likely to be important for transition metals with partially occupied d-shells. The applicability of potentials to clusters can be gauged by how well they reproduce surface structures and energies. The SC potential considerably underestimates surface energies and gives surface relaxations which are too large but which are qualitatively correct.²² The inclusion of directional terms in the Murrell–Mottram potential gives better surface energies than the SC potential, but the magnitudes of surface relaxations are slightly underestimated.²³

The global minima for MM and SC clusters Ni_{17-19} and Pt_{17-19} are compared in Fig. 9. The coordinates for the SC clusters were taken from the Cambridge Cluster Database of Wales and co-workers¹⁷ and these clusters have been discussed by Doye and Wales.²⁴ The same GM were predicted for Ni_{17-19} by Nayak *et al.*,²⁵ using the same SC potential. In all cases, except Ni_{19} , the MM and SC potentials predict different global minima. (The SC GM were reoptimised using the MM potentials to check that they did not in fact correspond to lower energy isomers than those already found.) For Pt, the SC GM for $N = 17$ and 18 correspond to the MM-derived isomers $\text{Pt}_{17}(3)$ and $\text{Pt}_{18}(5)$.

The double icosahedral isomer, which is the GM for Ni_{19} with both the MM and SC potentials has also been obtained as the GM in a recent study by Michaelian *et al.*, using a many-body Gupta potential,²⁶ which has a similar form to the SC

Table 11 Binding energies (eV) of the five most stable isomers found for M_{19}

M_{19}	Isomer				
	1 (GM)	2	3	4	5
Al	2.1890	2.1854	2.1821	2.1783	2.1778
Fe	2.5018	2.4535	2.4516	2.4508	2.4364
Ca	1.1664	1.1398	1.1397	1.1397	1.1296
Ni	2.8512	2.8406	2.8325	2.8293	2.8287
Pd	2.4361	2.3987	2.3966	2.3964	2.3919
Pt	3.8004	3.7914	3.7865	3.7862	3.7846

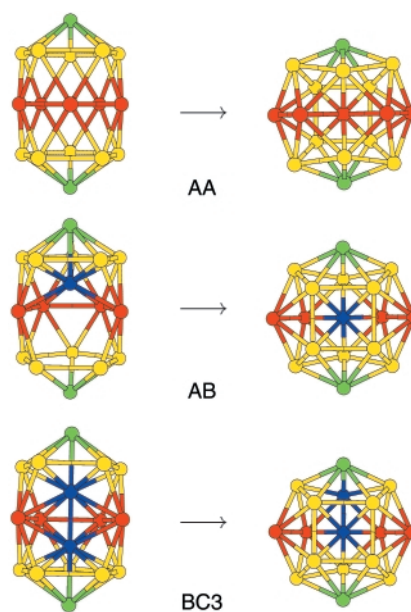


Fig. 7 Minimisation of M_{17} from different starting points resulting in the D_{4d} isomer.

potential. The SC GM for Ni_{17} and Ni_{18} are not among the five most stable MM isomers, but they appear closely related to the MM GM. Thus, the two “global minima” for Ni_{17} are related by a “diamond–square–diamond” rearrangement resulting in the formation of a bond (in the SC GM) between Ni atoms which are caps in the MM GM. The two “global minima” for Ni_{18} are also related by a C_{2v} -symmetry distortion, which involves the movement of the interstitial atom away from the centre of the cluster, so that it bonds to one of the capping atoms.

8.2 Lennard-Jones and Morse potentials

The global minima obtained for clusters with 17–19 atoms, bound by pairwise-additive Lennard-Jones (LJ) and Morse (Mor) potentials, are compared in Fig. 10. In the case of the Morse potential, two sets of clusters are shown: Mor(3) and Mor(14), corresponding to long ranged (Morse exponent = 3) and short ranged (Morse exponent = 14) Morse potentials. The GM were again obtained from the Cambridge Cluster Database.¹⁷

The ubiquitous double icosahedron is the GM for M_{19} clusters using the LJ and Mor(3) potentials—indicating that the stability of this isomer (which is the GM for all elements investigated in this study except for Pt) is due to the compact and highly-coordinated nature of the structure. The short-ranged Mor(14) potential finds capped decahedral structures as the GM for $N = 17-19$. As noted above, these structures are indeed the GM for Ni_{17} and Ni_{18} with the MM potential—which is consistent with the short-ranged character of both the 2-body ($a_2 = 8.5$) and the 3-body ($a_3 = 10$) components of the MM potential for nickel.

9 Conclusions

A detailed study has been presented of the low-energy isomers for 17–19-atom clusters of Al, Ca, Fe, Ni, Pd and Pt, bound by Murrell–Mottram 2 + 3-body potentials. These isomers have been found by the Random Search method. A systematic study has also been made of the relative stabilities, after local minimization, of isomers formed by removing one or two atoms from the double icosahedron, which is commonly predicted to be the global minimum for 19-atom clusters.

It has been shown that for a variety of metals, described by the Murrell–Mottram potential, all of the M_{18} isomers, generated by creating a vacancy in the M_{19} double icosahedron cluster, were found by the Random Search method. Three of the

fully relaxed IDI M_{18} clusters [$Pd_{18}(D)$, $Fe_{18}(D)$ and $Ca_{18}(C)$] were predicted to be global minima. It has also been proved that the GM for (MM) Fe_{18} and Ca_{18} were previously assigned incorrectly.^{13,14} In general, the fully relaxed IDI M_{18} structures were topologically very similar to the unrelaxed geometries, with the exception of $Pt_{18}(A)$ and $Pt_{18}(C)$, which underwent more substantial relaxation. In the case of the M_{17} IDI isomers, relaxation often leads to cluster rearrangement and the only unrelaxed IDI global minima are $Fe_{17}(CD1)$ and $Ca_{17}(AC1)$.

A common structural theme in the Al, Ni and Pt clusters is the appearance of relatively stable 4-fold symmetric structures (distorted capped Ino decahedra), which are the global minima for M_{17} and M_{18} for Al and Pt (and the second most stable isomers for Ni), the GM for Pt_{19} and the second most stable isomer for Al_{19} . The corresponding structure was not, however, found among the five most stable isomers of Ni_{19} . (Such structures are found at higher energies for Ca, Fe and Pd.) The distortion of the capped Ino decahedron corresponds to the breaking of an edge opposite to one of the caps¹⁵ on a square face and results in a cluster which lies half-way along a “diamond–square–diamond” rearrangement pathway. The other main structural feature observed for Ni MM clusters is the stability of undistorted tetracapped ($N = 17$) and pentacapped ($N = 18$)

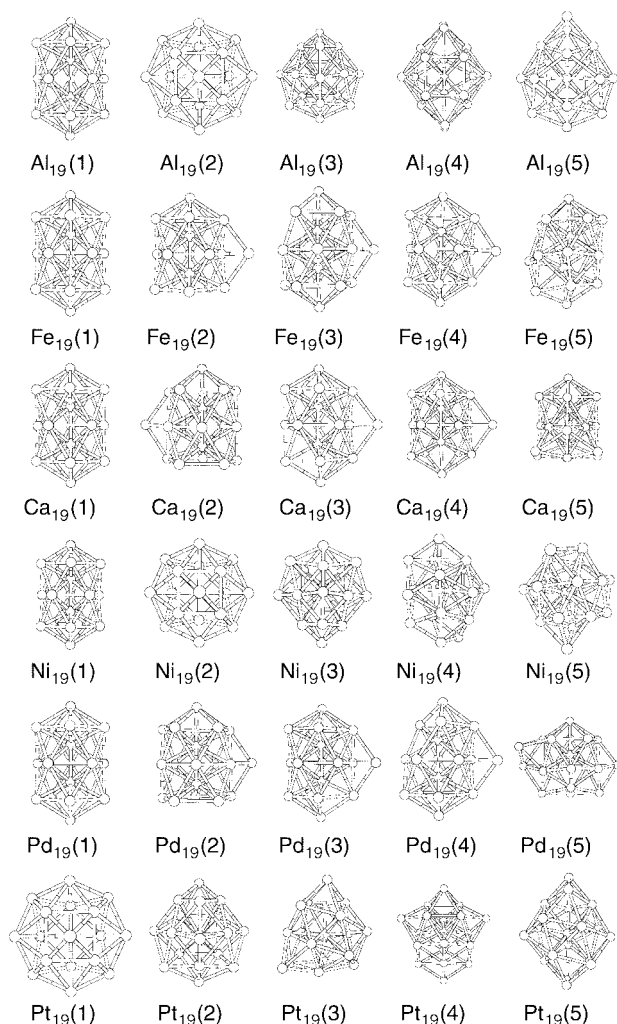


Fig. 8 The five most stable isomers found for M_{19} ($M = \text{Al, Ca, Fe, Ni, Pd and Pt}$).

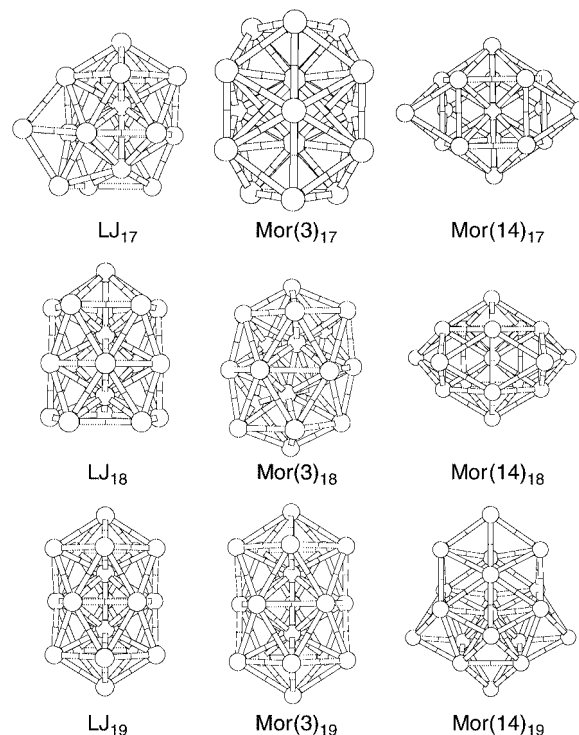


Fig. 10 Global minima for Lennard–Jones [LJ] and Morse [Mor(3) and Mor(14)] clusters with 17–19 atoms. (The number in parentheses is the range exponent of the Morse potential.)

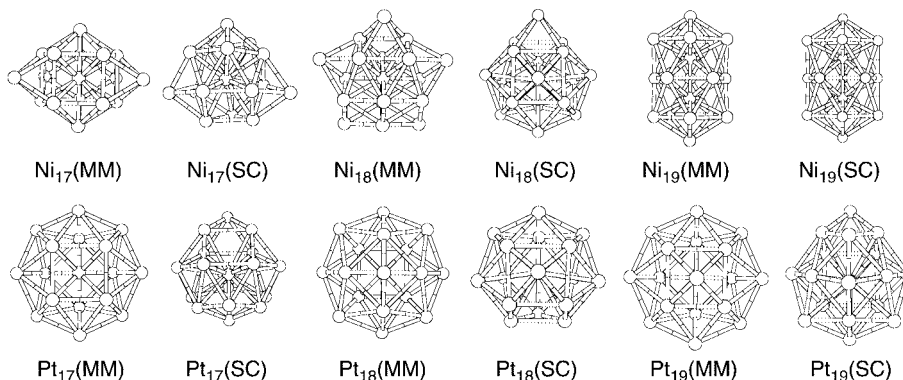


Fig. 9 Global minima for Murrell–Mottram [MM] and Sutton–Chen [SC] clusters of Ni and Pd with 17–19 atoms.

Ino decahedral clusters. This co-existence of undistorted and distorted capped Ino decahedra as minima on the potential energy surface has also been observed for Au clusters bound by the MM potential²⁰ and suggests low barriers to cluster fluxionality.

Comparison with previous studies has revealed many similarities between results obtained with the MM potentials and those using other many-body and pairwise-additive potential energy functions. The differences observed between the predicted low-energy isomers for the various elements also reflects differences found using alternative potentials. Doye and Wales, for example, have noted the differences between the GM found for Ni and Pt clusters studied with Sutton–Chen potentials.²⁴ More detailed studies of the structures, growth modes and dynamics of metal clusters are currently being undertaken over a wider size range. These studies will enable the MM potential to be tested against other potentials for its ability to reproduce experimentally observed cluster reactivity and fragmentation patterns.

The structures and coordinate files for the five lowest energy minima found for M_{17–19}, and for all the unrelaxed and relaxed IDI isomers, are available on the Birmingham Cluster Website.²⁷

Acknowledgements

The authors wish to thank Dr H. Cox (University of Sussex) for deriving the Murrell–Mottram potentials used in this study and Mr N. T. Wilson (University of Birmingham) for development of the CLUSPRO97 program and for his help in preparing the figures for this paper. Miss Hong Yao is also acknowledged for some preliminary calculations on Pd and Pt clusters. L. D. L. is grateful to the EPSRC for a Quota Studentship and R. L. J. acknowledges financial support from the Royal Society (RSRG/16180) and the University of Birmingham.

References

- 1 H. Haberland (Ed.), *Clusters of Atoms and Molecules*, Springer-Verlag, Berlin, 1994, p. 5.

- 2 T. P. Martin (Ed.), *Large Clusters of Atoms and Molecules*, Kluwer, Dordrecht, 1996.
- 3 R. L. Johnston, *Philos. Trans. R. Soc. London A*, 1998, **356**, 211.
- 4 S. Erkoç, *Phys. Rep.*, 1997, **278**, 80.
- 5 H. Cox, R. L. Johnston and J. N. Murrell, *J. Solid State Chem.*, 1999, **145**, 517.
- 6 J. N. Murrell and R. E. Mottram, *Mol. Phys.*, 1990, **69**, 571.
- 7 H. Cox, R. L. Johnston and J. N. Murrell, *Surf. Sci.*, 1997, **373**, 67.
- 8 J. E. Hearn, R. L. Johnston, S. Leoni and J. N. Murrell, *J. Chem. Soc., Faraday Trans.*, 1996, **92**, 425.
- 9 F. Gao, R. L. Johnston and J. N. Murrell, *J. Phys. Chem.*, 1993, **97**, 12073.
- 10 H. Cox, N. T. Wilson and R. L. Johnston, manuscript in preparation.
- 11 H. Cox, *Surf. Sci.*, 1998, **397**, 374.
- 12 R. L. Johnston and N. T. Wilson, CLUSPRO97, University of Birmingham, 1997.
- 13 N. A. Besley, R. L. Johnston, A. J. Stace and J. Uppenbrink, *Theor. Chem.*, 1995, **341**, 75.
- 14 J. E. Hearn and R. L. Johnston, *J. Chem. Phys.*, 1997, **107**, 4674.
- 15 L. D. Lloyd and R. L. Johnston, *Chem. Phys.*, 1998, **236**, 107.
- 16 NAG Fortran Library (Version 16), Numerical Algorithms Group, Oxford, 1993.
- 17 Cambridge Cluster Database, D. J. Wales, J. P. K. Doye, A. Dullweber and F. Y. Naumkin, URL <http://brian.ch.cam.ac.uk/CCD>.
- 18 J. P. K. Doye, D. J. Wales and R. S. Berry, *J. Chem. Phys.*, 1995, **103**, 4234.
- 19 N. T. Wilson and R. L. Johnston, manuscript in preparation.
- 20 N. T. Wilson and R. L. Johnston, *Eur. Phys. J.*, submitted.
- 21 A. P. Sutton and J. Chen, *Philos. Mag. Lett.*, 1990, **61**, 139.
- 22 B. D. Todd and R. M. Lynden-Bell, *Surf. Sci.*, 1993, **281**, 191.
- 23 J. Uppenbrink, R. L. Johnston and J. N. Murrell, *Surf. Sci.*, 1994, **304**, 223.
- 24 J. P. K. Doye and D. J. Wales, *New J. Chem.*, 1998, 733.
- 25 S. K. Nayak, S. N. Khanna, B. K. Rao and P. Jena, *J. Phys. Chem. A*, 1997, **101**, 1072.
- 26 K. Michaelian, N. Rendón and I. L. Garzón, *Phys. Rev. B*, 1999, **60**, 2000.
- 27 R. L. Johnston and N. T. Wilson, Birmingham Cluster Web, <http://www.tc.bham.ac.uk/beweb>

Paper a908003a